Food Chemistry 435 (2024) 137649

Contents lists available at ScienceDirect

Food Chemistry

journal homepage: www.elsevier.com/locate/foodchem

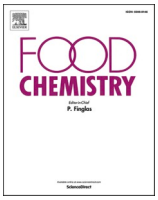

Electrochemistry of lyophilized blueberry and raspberry samples: ROS activation of the antioxidant ability of anthocyanins

Irene Domínguez [a,*], Irene Romero [b], M. Teresa Sanchez-Ballesta [b], M. Isabel Escribano [b], Carmen Merodio [b], Antonio Doménech-Carbó [c,*]

[a] Department of Agroindustry and Food Quality, Andalusian Institute of Agricultural and Fisheries Research and Training (IFAPA), La Mojonera, Camino San Nicolás, 1, Almeria E-04745, Spain
[b] Department of Characterization, Quality and Safety, Institute of Food Science, Technology and Nutrition (ICTAN-CSIC), Ciudad Universitaria, E-28040 Madrid, Spain
[c] Department of Analytical Chemistry, University of Valencia, Dr. Moliner 50, 46100 Burjassot, Valencia, Spain

ARTICLE INFO

Keywords:
Blueberry
Raspberry
Lyophilized
Electrochemistry
ROS

ABSTRACT

An electrochemical study of lyophilized blueberry (*Vaccinium corymbosum L.*) and raspberry (*Rubus idaeus* L.) fruits was carried out using microparticulate deposits from ethanolic extracts of fruits in contact with different aqueous electrolytes. This voltammetry is dominated by the oxidation of anthocyanins. It was hypothesized that under conditions of electrochemical generation of reactive oxygen species (ROS), new anthocyanin-derived species with high antioxidant capacity are formed over a wide pH range. In the case of ROS-activated anthocyanins, electrochemical oxidation is associated with loss of sugar moieties. Experimental voltammetric and scanning electrochemical microscopy (SECM) imaging data consistent with this hypothesis are presented.

1. Introduction

Berries have interesting antioxidant properties due to their abundance of anthocyanins and other bioactive compounds (Cesa et al., 2017; Mustafa et al., 2022). Anthocyanins, polyphenolic components attributed to the flavonoid family, play an important role in protecting higher plants from photochemical and biochemical damage (Yi et al., 2012; Dimitrić Marković et al., 2017). These compounds are known for their high antioxidant capacity and have been associated with beneficial health effects, such as reduced risk of cancer and cardiac diseases (Garcia & Blesso, 2021; Olson et al., 2021).

Due to their specific structural characteristics, anthocyanins have the ability to scavenge radicals, including superoxide radicals and other reactive oxygen species (ROS) (Fan, Lin, Zhang, Li, & Tang, 2023; Cerqueira et al., 2023). In fact, the radical scavenging capacity of anthocyanins in berries has recently been studied with respect to thermal processing of blueberry puree (Kim et al., 2021), in vitro-simulated digestion (Lang et al., 2021), and physiological and biochemical changes during fruit ripening (Shi et al., 2023). The currently accepted view is that anthocyanins and flavonoids in general, donate hydrogen atoms from phenoxyl groups to radicals, thereby inactivating their oxidative activity. These processes are usually described in terms of three alternative mechanisms, hydrogen atom transfer (HAT), sequential proton loss electron transfer (SPLET), and single electron transfer followed by proton transfer (SET-PT) (Litwinienko & Ingold, 2007).

In this context, we recently studied the *in situ* electrochemistry of fresh blueberry (*Vaccinium corymbosum L.*, fam. Ericaceae) fruits and obtained a seemingly surprising result: the anthocyanidin-localized voltammetric response was sensitive to the presence of ROS (Doménech-Carbó & Domínguez, 2023). Therefore, the current work is based on the hypothesis that, under conditions of electrochemical generation of ROS, new anthocyanin-derived species with high antioxidant capacity are formed. This is accompanied by three additional hypotheses: i) not only anthocyanidins (aglycones), but also anthocyanins display the above response; ii) the anthocyanin-derived species with low oxidation potential are formed in a wide range of pH values; iii) they are formed in anthocyanins not only from fresh blueberry but also from lyophilized blueberry and raspberry fruits.

This is of potential interest in food chemistry as the results obtained paint a relatively complex picture of the interaction between anthocyanins and ROS. Apart from their known role as radical scavengers via phenoxide intermediates (Litwinienko & Ingold, 2007), anthocyanins may act as promoters of the generation of new and potent antioxidants via reaction with ROS.

* Corresponding authors.
E-mail addresses: irene.dominguez.perez@juntadeandalucia.es (I. Domínguez), antonio.domenech@uv.es (A. Doménech-Carbó).

https://doi.org/10.1016/j.foodchem.2023.137649
Received 1 August 2023; Received in revised form 29 September 2023; Accepted 30 September 2023
Available online 4 October 2023

Therefore, the aim of this work was to verify the occurrence of this phenomenology in different types of lyophilized red berries. For this purpose, blueberry, and raspberry (*Rubus idaeus* L., fam. Rosaceae) fruits were selected according to their high anthocyanin content and high consumption. This makes the study of interest for other potential applications (Slika et al., 2022) and plant physiology related to plant defense against different types of stress and the corresponding signaling (Wasternack & Hause, 2013; Zhou, Li, Zhao, Deng-Wang, & Dai, 2016).

The electrochemistry of polyphenolic compounds, and flavonoids in particular, has received much attention in both aqueous and non-aqueous electrolytes. In aqueous solution at and near biological pHs (7.0–7.4), the main voltammetric signal of flavonoids with having o-catechol units (such as quercetin and pelargonidin) has been attributed to the 2-proton, 2-electron oxidation of these units to the corresponding o-quinones. These are multistep processes involving proton and electron transfers that correspond to chemical (C) plus electron transfer (E) sequences of ECEC or CECE types. Furthermore, this process can often be accompanied by the oxidation of the 5,7-dihydroxyl groups, which occurs at higher potentials (Ramesova, Sokolova, Tarabek, & Degano, 2013; Masek, Chrzescijanska, & Zaborski, 2014; Arroyo-Currás, Rosas-García, & Videa, 2016; Yang, Yang, Li, Ma, & Yu, 2022) and, in the case of anthocyanins, by ring opening oxidations (Janeiro & Oliviera-Brett, 2007). In contrast, few electrochemical studies have been devoted to the interaction of flavonoids with ROS, focusing on the reversible generation of superoxide radical anions in organic solvents (Lauw, Chiang, Lee, & Webster, 2018; Jadreško, Miličević, & Novak Jovanović, 2022).

In this context, we have directly applied an electrochemical methodology inspired by voltammetry of immobilized particles (VIMP), a technique focused on the analysis of sparingly soluble materials (Scholz, Schröder, Gulabowski, & Doménech-Carbó, 2014) to the study of plant materials. This consists in recording the voltammetric response, in contact with aqueous electrolyte solutions, of microparticulate deposits resulting from the evaporation of extracts of leaves, seeds, etc. in organic solvents. This strategy was previously used to characterize plant varieties as well as extract chemotaxonomic and phylogenetic information (Doménech-Carbó et al., 2015; Mateo et al., 2018).

The insertion of macro- (Doménech-Carbó, Domínguez, Hernández, & Gavara, 2015) and microelectrodes (Doménech-Carbó, Dias, & Donnici, 2021) in fruits and leaves also allowed successful *in situ* analyses of intact fruit samples. The voltammetric responses obtained were focused on the oxidation of polyphenolic compounds occurring at physiological pHs in the region of potentials between 0.0 and 1.2 V vs. Ag/AgCl. However, working with air-saturated electrolyte solutions and prolonging the potential scan to more negative values will lead to the generation of ROS as a result of the reduction of dissolved oxygen. This strategy was previously used to study the reactivity of phenolic compounds present in different tomato varieties with ROS (Doménech-Carbó, Gavara, Hernández-Muñoz, & Domínguez, 2015), later used in the plant physiology and phylogenetics studies.

Air-saturated and progressively deaerated electrolyte solutions at physiological pH were used, optionally adding DMSO due to its radical scavenger properties (Herscu-Kluska, Masanwa, Saphier, Cohen, & Meverstein, 2008). The voltammetric study is complemented by the analysis of cyanidin, pelargonidin, and peonidin 3-glucoside standards. Cyanidin and peonidin glycosides were the majority species identified in the lyophilized samples studied here. In addition, scanning electrochemical microscopy (SECM) data recorded on thin sections of lyophilized blueberry fruits were used to confirm the 'local' interaction of anthocyanins with electrochemically generated ROS.

2. Experimental

2.1. Plant material

Blueberry (cv. Duke) and raspberry (cv. Regina) fruits were collected in Salas (Asturias, Spain) in June 2022. The fruits were transported to the ICTAN-CSIC center (Madrid, Spain) on the same day of collection and 3 pools of 250 g of fruits without mechanical or pathological defects were frozen in liquid nitrogen, blended, and finally stored at −80 °C. For the voltametric measurements the samples were subsequently lyophilized.

2.2. Sample preparation and anthocyanin characterization by HPLC-QTOF-MS/MS analyses

Anthocyanin extraction was performed on three biological replicates, each sample consisting of 0.2 g (from a pool of 250 g) of frozen blueberry and raspberry samples, stored at − 80 °C. For each extraction, the 0.2 g of sample was mixed with 1 mL of acidified methanol (50:50 v/v, 1% HCl:water) and stirred at 200 rpm for 1 h at room temperature. Finally, the supernatant was extracted after centrifugation (10,000*g*, 10 min). This procedure was performed twice, so that after mixing both supernatants, the final extract was filtered through 0.45 μm nylon filters and stored at −20 °C until analysis.

Anthocyanins profile was analyzed using high resolution chromatography equipment with Quadrupole Mass Spectrometer-Time of Flight (HPLC-QTOF). Concretely, analyses were performed using an Agilent 1200 Liquid Chromatograph (Agilent Technologies, Waldbronn, Germany), composed of a quaternary pump (G1311A) with an integrated degasser trailer (G1322A), a thermostated automatic injector (G1367B) and a thermostated column module (G1316A) coupled in series to an accurate-mass quadrupole time-of-flight (Q-TOF) LC-MS (Agilent G6530A), with ionization source at atmospheric pressure electrospray (ESI) Jet Stream Technology (Agilent Technologies, Waldbronn, Germany). Samples were injected refrigerated, and the components were separated using an Agilent Zorbax Eclipse XDB-C18 (150 × 4.6 mm, 5 μm) column at 40 °C. The mobile phase consisted of acidified water containing 0.1% formic acid (v/v, A) and acetonitrile with 0.1% formic (B). The gradient used started with 5% phase B at time 0, 30% at 30 min, 5% at 45 min. The flow rate was 1 mL/min, and the instrument was operated in positive ion polarity mode and extended dynamic range (1700 *m/z*, 2 GHz).

Anthocyanin peaks were identified from an in-house database containing chromatographic and mass spectrometric information such as retention time, parent theoretical mass and confirmation/characteristic fragments (data summarized in Table S1). For compound quantification malvidin 3-glucoside ($C_{23}H_{25}O_{12}$) was used as external standard. The calibration curve ranged from 1.2 to 20 ppm, using the same solvent as in the extraction procedure (50:50 v/v, 1% HCl:water). The results were then expressed as mg 100 g^{-1} fresh weight (FW). Three replicates were analyzed in each case. The software used were MassHunter Data Acquisition B.05.01 and MassHunter Qualitative Analysis B.07.00 SP2 from Agilent.

Descriptive analyses were performed using the IBM-SPSS statistics program, version 28.0.0 (IBM Corp. Armonk, NY, USA). Differences between the anthocyanin contents of blueberries and raspberries were determined by one-way analysis of variance (ANOVA) and the Tukey-B test ($p \leq 0.05$).

2.3. Electrochemical measurements

Prior to the electrochemical analysis, samples were lyophilized. For this purpose, 5 g of the each of the three frozen samples (3 biological replicates) were lyophilized in a Beta 2–8 LDplus freeze dryer from Christ (Apeldoorn, The Netherlands) operating at −65 °C and 0.0054 mbar for 96 h. Subsequently, the samples were homogenized by grinding in a Mixer Mill MM 200 (2 min at 25 r/s) and stored in desiccators until analysis. From the different pools, three biological replicates were obtained and analyzed.

Voltammetric measurements were performed on: i) solutions of anthocyanin standards in different aqueous electrolytes, and ii) glassy carbon electrodes (GCEs) modified with films of the lyophilized fruits. A

conventional three-electrode arrangement was used including the unmodified and sample-modified GCE as the working electrode, a Ag/AgCl (5 M NaCl) reference electrode, and a Pt-wire auxiliary electrode. Measurements were performed at room temperature (298 ± 2 K) using 0.10 M potassium phosphate buffer at pH 7.4, 0.25 M HAc/NaAc buffer at pH 4.75, 0.10 M H_2SO_4 and 0.10 M KOH as electrolyte solutions. The cell was optionally deaerated by bubbling Ar for 10–15 min. Cyanidin, pelargonidin, and peonidin 3-glucoside standards (Fluka) were used as received to prepare solutions of concentration ca. 0.5 mM in the above electrolytes. Experiments in DMSO solution (Carlo Erba) were carried out using Bu_4NPF_6 (Fluka) as a supporting electrolyte and a Pt-wire pseudoreference electrode. In this case, ferrocene was used as internal standard for potential measurements. The potentials in the text are referred to Ag/AgCl after calibration with ferrocene.

Sample-modified working electrodes were conditioned by evaporating at air one drop (20 μL) of the suspension resulting from the maceration of ca. 50 mg of lyophilized sample with 0.5 mL of ethanol in an agate mortar. Three replicate experiments were performed for each lyophilized sample. Complementary experiments were carried out on films of the standards on GCE obtained by evaporation in air of 50 μL of ethanolic solutions (ca. 0.5 mM) of the respective compounds.

All electrochemical measurements were carried out with a CH 920c potentiostat (Cambria Scientific, Llwynhendy, Llanelli UK). Cyclic voltammograms at potential scan rates between 10 and 500 V s^{-1} and square wave voltammograms at frequencies between 5 and 500 Hz were recorded.

SECM experiments were performed on thin films of lyophilized blueberry and raspberry fruits (surface area ca. 1–2 mm^2), cut with a scalpel. The freshly cut films were adhered to a bed (geometrical area 0.785 cm^2) of graphite paste (50% wt graphite plus 50% wt nujol oil) covering a Pt substrate (geometrical area 0.019 cm^2) electrode. A 20 μm diameter Pt microelectrode was used as the tip electrode, with its edge at a distance from the substrate of the order of the tip radius. The scanning rate of the tip over the substrate was 20 μm s^{-1}. The redox probe was a 2.5 mM $K_3Fe(CN)_6$ plus 2.5 mM $K_4Fe(CN)_6$ solution in 0.10 M potassium phosphate buffer at pH 7.4. The probe approach curves and SECM images were obtained by applying a constant potential of 0.30 V vs. Ag/AgCl to the tip electrode. This potential corresponds to the oxidation of $Fe(CN)_6^{4-}$ to $Fe(CN)_6^{3-}$ under diffusion-controlled conditions.

3. Results and discussion

3.1. Compositional study

Analysis of the berry samples by means of HPLC-Q-TOF-MS/MS revealed the presence of several anthocyanins whose MS signatures and concentrations in the fruit are summarized in Table 1. Significant differences were observed between them, as different compounds were identified in each case. In blueberries, malvidin-3-arabinoside, malvidin-3 galactoside, peonidin-3-arabinoside, peonidin-3-glucoside and peonidin-3-galactoside were the anthocyanins found, with arabinosides being a minority, in contrast to a recent study which showed the presence of delphinidin and petunidin glycosides in addition to malvidin glycosides, (Shi et al., 2023). In terms of the glycosylated form, the arabinoside and galactoside malvidins are present in comparable proportions, while the glucoside was the predominant form of peonidin.

As shown in Table 1 for raspberry fruit cyanidin glycosides where the anthocyanins identified in the samples. Consistent with previous studies (Mihailović et al., 2019), among the cyanidin glycosides, the highest content was associated to cyanidin-3-sophoroside, followed by cyanidin-3-2G-glucosylrutinoside, cyanidin-3-glucoside, and finally cyanidin-3-rutinoside.

3.2. Voltammetric pattern

Fig. 1 shows the square wave voltammograms of microparticulate deposits from ethanolic extracts of lyophilized blueberry deposited on GCE in contact with 0.25 M HAc/NaAc aqueous buffer at pH 4.75 when the potential scan was initiated at −1.05 V vs. Ag/AgCl in the positive direction. In deoxygenated solutions, the voltammogram consists of a series of overlapping anodic peaks between −0.2 and 0.8 V (labeled as I-peaks). For air-saturated solutions, the voltammograms show a similar profile in this region of potentials but are preceded by an additional, prominent oxidation peak at −0.7 V (labeled as II). This signal is absent for unmodified GCEs in air-saturated solutions, as well as for H_2O_2 in the same and other electrolytes tested, indicating that it cannot be attributed to any oxygen species, i.e., that the electrochemical process is

Table 1
Anthocyanin content in raspberry cv. Regina and blueberry cv. Duke and MS parameters of the anthocyanins found in the samples studied[a].

Anthocyanins	Formula	Molecular Weight	M + H	mg 100 g^{-1} FW
Raspberries (cv. Regina)				
Cyanidin 3-glucoside	$C_{21}H_{21}O_{11}$	449.3848	450.1154	12.95 ± 0.64c
Cyanidin 3-sophoroside	$C_{27}H_{31}O_{16}$	611.5254	612.1682	92.98 ± 2.54a
Cyanidin 3-2G-glucosylrutinoside	$C_{33}H_{41}O_{20}$	757.6666	758.2261	25.04 ± 0.82b
Cyanidin-3-rutinoside	$C_{27}H_{31}O_{15}$	595.5260	596.1733	1.326 ± 0.30d
Blueberries (cv. Duke)				
Malvidin 3-arabinoside	$C_{22}H_{23}O_{11}$	463.4114	464.1310	1.46 ± 0.04a
Malvidin 3-galactoside	$C_{23}H_{25}O_{12}$	493.4374	494.1416	1.48 ± 0.04a
Peonidin 3-arabinoside	$C_{21}H_{21}O_{10}$	433.3854	434.1205	1.39 ± 0.02a
Peonidin 3-glucoside	$C_{22}H_{23}O_{11}$	463.4114	464.1310	1.35 ± 0.02a
Peonidin 3-galactoside	$C_{22}H_{23}O_{11}$	463.4114	464.1310	1.40 ± 0.02a

[a] Values are mean of three replicates ± standard deviation. Different letters within the same fruit indicate significant differences ($p < 0.05$).

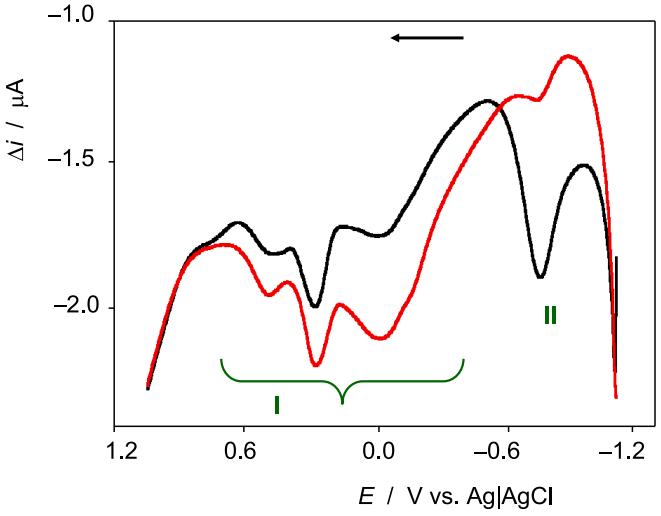

Fig. 1. Square wave voltammograms of microparticulate deposits from ethanolic extracts of lyophilized blueberry deposited on a GCE in contact with: a) air-saturated (red), and b) deoxygenated (black) 0.25 M HAc/NaAc aqueous solutions at pH 4.75. Potential scan initiated at 1.05 V vs. Ag/AgCl in the positive direction; potential step increment 4 mV; square wave amplitude 25 mV; frequency 5 Hz. The arrow indicates the direction of the potential scan. (For interpretation of the references to color in this figure legend, the reader is referred to the web version of this article.)

anthocyanidin-localized.

Similar general behavior was obtained in 0.10 M potassium phosphate buffer at pH 7.4 (see Supplementary Information, Fig. S1), and 0.10 M H_2SO_4. Although the profile of the I-signals varied, in all cases the signal II disappeared in O_2-free solutions. The extracts of lyophilized raspberry samples showed a completely comparable electrochemistry, which in turn reproduced the features recorded *in situ* with platinum microelectrodes inserted in blueberry fruits (Doménech-Carbó and Domínguez, 2023). Interestingly, a similar response was obtained in 0.5 mM solutions of cyanidin, pelargonidin, and peonidin 3-glucoside (see Supplementary Information, Fig. S2), suggesting that the peculiar II voltammetric features may be related to the anthocyanins. The voltammetry of lyophilized raspberry extracts in 0.10 M KOH electrolytes showed, as can be seen in Fig. 2a, a more complicated profile, with two II peaks at −0.50 and −0.70 V, as before, which progressively disappear upon deoxygenation of the electrolyte solution (see also Supplementary Information, Fig. S3). As the potential scan is initiated at increasingly negative potentials (see Fig. 2b), the II profile becomes progressively more and more complicated. On the contrary, in air-saturated 0.25 M HAc/NaAc and 0.10 M H_2SO_4 solutions, the II signal remains as a unique, isolated peak for both raspberry (Fig. 2c) and blueberry (Fig. 2d) samples.

To rationalize this behavior, it should be noted that the 'ordinary' electrochemistry of anthocyanins has been described in the potential region from 0.0 to 1.2 V (De Lima, Sussuchi, & De Giovanni, 2007), which is very similar to that of all other flavonoids (Ramesova, Sokolova, Tarabek, & Degano, 2013; Masek, Chrzescijanska, & Zaborski, 2014; Arroyo-Currás, Rosas-García, & Videa, 2016). As mentioned above, this electrochemistry is centered on the oxidation of *o*-catechol units to *o*-quinones in both aqueous and nonaqueous media.

In turn, the reduction of dissolved oxygen occurs under our experimental conditions at potentials between − 0.5 and − 0.9 V. This is a complex, multistep process whose first step is the one-electron formation of the radical anion superoxide with subsequent formation of the radicals hydroperoxide and hydroxyl, H_2O_2 and, finally, H_2O (Xu, Huang, & McCreery, 1996; Katsounaros et al., 2012).

As discussed below, the anthocyanins can react with the electrochemically generated superoxide radical anion. This can be clearly seen in aprotic media, where dissolved oxygen undergoes a reversible one-electron reduction to the superoxide radical anion:

$$O_2 + e^- \rightarrow O_2^{\bullet -} \quad (1)$$

The interaction between the anthocyanins and the nascent superoxide radical anion is illustrated by the cyclic voltammograms shown in Fig. 3. The upper part of this figure (Fig. 3a) shows the voltammogram recorded on a cyanidin film on a GCE immersed in an air-saturated 0.10 M Bu_4NPF_6/DMSO solution. The voltammogram is dominated by the reduction of dissolved oxygen at ca. − 0.9 V vs. Ag/AgCl, which appears as two overlapping signals (C_{ox}). In the subsequent anodic scan, there no oxidation peaks coupled to the previous reduction ones. Under these conditions, the anthocyanin-localized oxidation signals (I) become much less intense. This response is in abrupt contrast to the voltammograms at the bare GCE (Fig. 3b), where a unique cathodic peak (C_{ox}) is coupled to a well-defined anodic peak (A_{ox}). This pattern is maintained as more negative potentials are reached (see superimposed voltammograms in Fig. 3b). In agreement with the literature in the solution phase (Lauw, Chiang, Lee, & Webster, 2018; Jadreško, Miličević, & Novak Jovanović, 2022), the 'ordinary' anthocyanidin signals (A) are

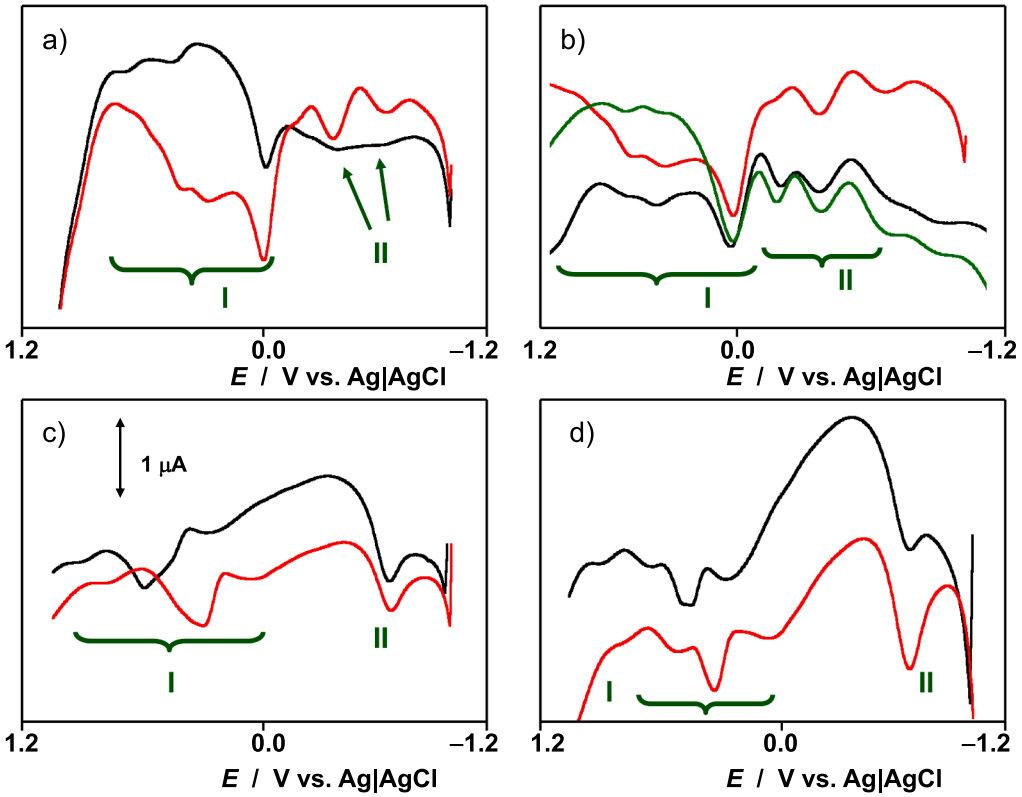

Fig. 2. A,b) Square wave voltammograms of microparticulate deposits from ethanolic extracts of lyophilized raspberry deposited on a gce in contact with: 0.10 M KOH aqueous solution; a) potential scan initiated at − 1.15 V in the positive direction; deoxygenated (black line) and air-saturated (red line) solutions; b) detail of voltammograms initiated at − 1.05 (red), −1.25 (green), and − 1.45 V (black) in the positive direction. c,d) square wave voltammograms of lyophilized raspberry; (c) and blueberry and (d) extracts in contact with 0.10 M H_2SO_4 (black lines) and 0.25 M HAc/NaAc (pH 4.75, red lines)) solutions. Potential step increment 4 mV; square wave amplitude 25 mV; frequency 5 Hz. (For interpretation of the references to color in this figure legend, the reader is referred to the web version of this article.)

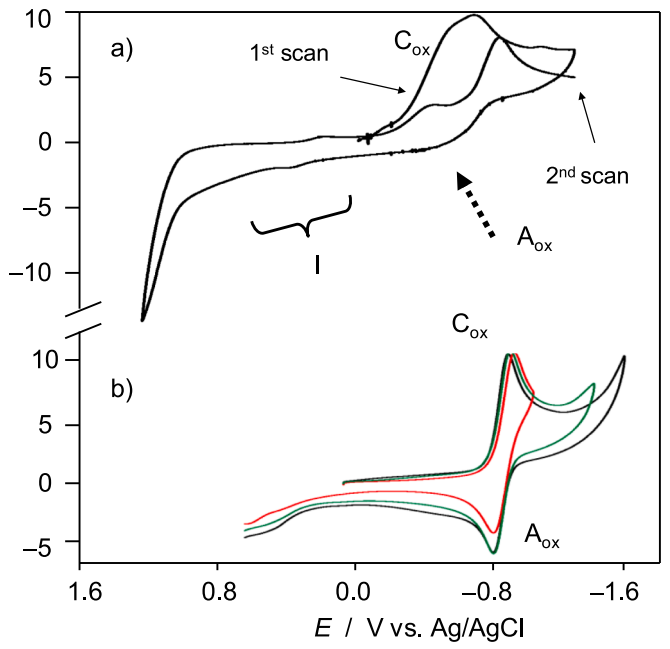

Fig. 3. Cyclic voltammograms recorded in air-saturated 0.10 M Bu_4NPF_6/DMSO solutions on: a) cyanidin film deposited on GCE, and b) bare glassy carbon electrode. Potential scan initiated at 0.0 V vs. Ag/AgCl in the negative direction: potential scan rate 50 mV s^{-1}. The first and second cathodic scans are marked in (a), while three voltammograms with different switching potentials are superimposed in (b). The dotted arrow marks the absence of A_{ox} signal in (a).

only slightly modified.

The voltammetric data in Fig. 3a can be interpreted under the assumption that the superoxide radical anion generated in the C_{ox} process (Eq. (1)) reacts rapidly with the anthocyanin so that the reverse of Eq. (1) does not occur. In aprotic media, under our experimental conditions, this process regenerates O_2,

$$\text{Ar-OH}^{+} + O_2^{\bullet -} \rightarrow \text{Ar-OH} + O_2 \quad (2)$$

promoting its reduction at less negative potentials. This regenerative (catalytic) pattern gives rise to the split in peak C_{ox} (Fig. 3a). As the anthocyanin film is depleted, peak A_{ox} reappears, as can be seen in the second negative-going potential scan of the voltammogram in Fig. 3a. The process represented by Eq. (2) can be viewed as the formation of a semiquinone radical with the abstraction of one proton.

In the presence of water, the reaction of anthocyanins with superoxide radical anion involves the formation of phenoxyl radical and hydrogen peroxide. A scheme of the 'ordinary' aqueous electrochemistry of anthocyanidins using cyanidin as a representative example of this group of compounds is illustrated in Fig. S4. The scheme includes the scavenging of the radical anion superoxide by the intermediate phenoxyl radical, which exemplifies the currently accepted pathway for ROS abstraction. For our purposes, it is important to emphasize that the interaction with ROS in aprotic media leads to modifications of the 'ordinary' flavonoid signals but not to new voltammetric signatures. Eventually, the electrochemically generated ROS can react with flavonoids such as quercetin to form new electroactive species. As a result, the I-region of the voltammograms changes when the scan is initiated at potentials sufficiently negative to cause the reduction of dissolved oxygen (Doménech-Carbó, Gavara, Hernández-Muñoz, & Domínguez, 2015; Doménech-Carbó, Montoya, Soriano, & Estrelles, 2018).

Accordingly, the II signal(s) can be attributed to a species generated by the reaction of the parent anthocyanin with electrochemically generated ROS. Consistent with this hypothesis, the height of this signal decreases with decreasing the measurement time (i.e., increasing the potential scan rate in linear sweep voltammetry or increasing the frequency in square wave voltammetry) and increases with starting the potential scan at more negative potentials.

3.3. SECM imaging

In order to evaluate the differences between I and II voltammetric signals, SECM experiments were performed on thin films of lyophilized blueberry and raspberry fruits adhered to a graphite paste bed as a substrate electrode. This was placed in contact with $Fe(CN)_6^{3-}/Fe(CN)_6^{4-}$ redox probe in air-saturated 0.10 M potassium phosphate buffer at pH 7.4, in which the Pt-tip microelectrode was immersed. By applying different potential inputs to the substrate electrode using the redox competition strategy (Karnicka et al., 2007), it is possible to detect changes in the topography and conductivity of the films (Doménech-Carbó and Domínguez, 2023). The color plot in Fig. 4a corresponds to the boundary between the insulating fruit film (denoted by the green negative feedback area) and the more conductive graphite paste (brown area), recorded when the tip potential (E_T) was fixed at 0.4 V where the redox probe is reversibly oxidized under diffusion-controlled conditions.

The corresponding topographic image in Fig. 4b shows a layered fruit area with peaked features at the boundary with the carbon paste. When a potential capable of producing I-signals was applied to the substrate (E_S = 0.6 V), the boundary region increased the number of peaked features, while the fruit area retained its layered appearance but was slightly smoothed (Fig. 4c). These features can be interpreted on assuming that the boundary region, where a cross-section of the fruit layer was exposed to the electrode, concentrates the area where the electroactive components of the plant exchange protons and electrons with the base carbon paste electrode and the electrolyte solution. This is the expected behavior according to the three-phase electrochemistry that characterizes solid state processes (Scholz & Meyer, 1998; Scholz, Schröder, Gulabowski, & Doménech-Carbó, 2014; Doménech-Carbó, Labuda, & Scholz, 2013).

When a potential of −1.0 V is applied to the substrate (Fig. 4d), there are significant changes in the electrochemical topography. Now, the film/base electrode junction becomes less irregular, albeit with peaked features, while the appearance of the fruit film area changes dramatically. The layered surface structure is now intersected by transverse positive feedback features. This suggests that the application of a ROS-generating potential to the substrate electrode largely determines the localized reaction with plant constituents. Since SECM experiments require ca. 5 min of application of the ROS-generating potential, this relatively long exposure increases the extent of the putative ROS-anthocyanin reactions. This is in agreement with the observation that the intensity of the II signals increases with decreasing frequency in square wave voltammetric measurements. Comparable results were obtained for raspberry samples (see Supplementary Information, Fig. S5).

3.4. Discussion

The interaction of ROS with phenolic compounds has been extensively studied in aprotic solvents (Lauw, Chiang, Lee, & Webster, 2018; Jadreško, Miličević, & Novak Jovanović, 2022), where the superoxide radical anion generated by the one-electron reversible reduction of O_2 is stabilized on the time scale of voltammetric experiments. The superoxide-scavenging activity of flavonoids (and anthocyanins in particular) involves the reaction of ROS with the phenolic moiety (Ar-OH) (Dimitrić Marković et al., 2017). This process can be represented as either.

$$O_2^{\bullet -} + \text{Ar-OH} \rightarrow HO_2^{\bullet} + \text{Ar-O}^{-} \quad (3)$$

or

$$O_2^{\bullet -} + \text{Ar-OH} \rightarrow HO_2^{-} + \text{Ar-O} \quad (4)$$

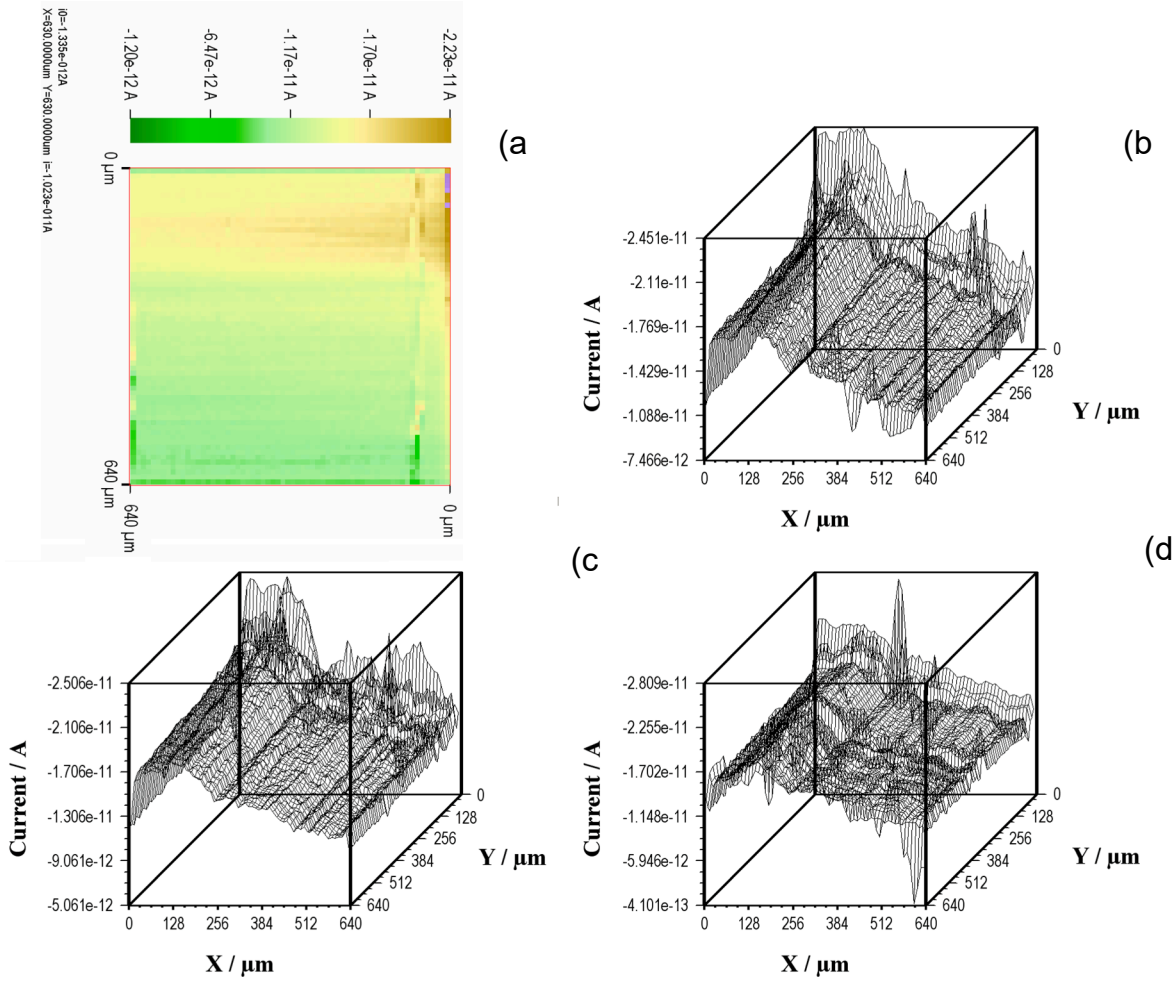

Fig. 4. SECM study of a thin film of lyophilized blueberry fruit adhered to a graphite paste bed deposited on a Pt electrode in contact with 2.5 mM $K_3Fe(CN)_6$ plus 2.5 mM $K_4Fe(CN)_6$ solution in air-saturated 0.10 M potassium phosphate buffer at pH 7.4. The potential applied to the tip was of 0.30 V vs. Ag/AgCl. a) color plot for $E_S = 0$; b-d) topographic images for b) $E_S = 0.0$ V, c) $E_S = 0.6$ V, d) $E_S = \square 1.0$ V.

As a result of the hydrogen donation from a flavonoid phenoxy group to the radicals, ROS radicals are inactivated while phenoxyl radicals or anions, less reactive and more stable species are formed.

Alternatively, phenoxide radicals and/or anions may be formed during the 'ordinary' stepwise electrochemical oxidation of flavonoids,

$$\text{Ar-OH} \rightarrow \text{Ar-O}^{\bullet} + \text{H}^{+} + \text{e}^{-} \quad (5)$$

$$\text{Ar-O}^{\bullet} \rightarrow \text{Ar-O}^{-} + \text{H}^{+} + \text{e}^{-} \quad (6)$$

For polyphenolic compounds these processes lead to the formation of quinones. These processes, which are schematized in Fig. 5 for cyanidin, correspond to the I signals in Figs. 1 and 2. In cases such as pelargonidin, cyanidin, delphinidin, quercetin, etc. oxidation of *o*-catechol units to the corresponding *o*-quinones occurs. In the case of anthocyanidins and anthocyanins, the electrochemical oxidation can also occur at more positive potentials within the I-region involving reaction with water and ring opening (Janeiro & Oliviera-Brett, 2007). This type of process is illustrated in Fig. 5. Replacement of hydroxyl units with methoxy groups, or the addition of a glucoside results in an anodic shift of the oxidation potentials, i.e., a decrease in antioxidant activity. However, this activity also depends on a different set of factors (Sinopoli, Calogero, & Bartolotta, 2019; Dong et al., 2023).

This scene is, in principle, applicable to aqueous solution under conditions of electrochemical ROS generation. Here, however, the superoxide radical anion generated in the first step of O_2 reduction undergoes subsequent chemical and electrochemical reactions. As a result, several reactive species ($HO_2^{\bullet}$, $HO^{\bullet}$, H_2O_2) can be formed, depending on the experimental conditions. Assuming, for simplicity, that superoxide is the main ROS, there is the possibility of different reaction pathways coupled to voltammetric experiments. A first possibility is the formation of peroxo bridges as described for quercetin (Krishnamachari, Levine, & Paré, 2002). The resulting species can also be electrochemically oxidized leading to new signals in the I-region of the potentials (Doménech-Carbó, Gavara, Hernández-Muñoz, & Domínguez, 2015).

It is conceivable that these species do not provide the sufficiently high degree of electronic conjugation proposed to be necessary to explain the high negative value of the potential of the signal II. The anthocyanins are arranged as a phenyl ring (ring A) fused with a pyran ring (ring C), in addition to another phenyl ring (ring B) substituted at position 2 of ring C. In the 'ordinary' electrochemistry (signals labeled as A in the voltammograms) of anthocyanins, the OH group in the position 3 of the ring C is blocked with sugar moiety. Then, the electrochemical oxidation involves the *o*-catechol units in the ring B. Under previous activation by electrochemically generated ROS, the oxidation of anthocyanins can lead to species with high degree of conjugation by releasing the sugar unit. This is schematized in Fig. 5 for the case of cyanidin-3-glucoside (grey zone). The loss of the sugar moiety is consistent with the removal of this unit occurring during thermal degradation of anthocyanins (Sadilova, Stintzing, & Carle, 2006; Duan et al., 2024). Of course, since several ROS can be generated depending on the experimental conditions, different reaction pathways can operate.

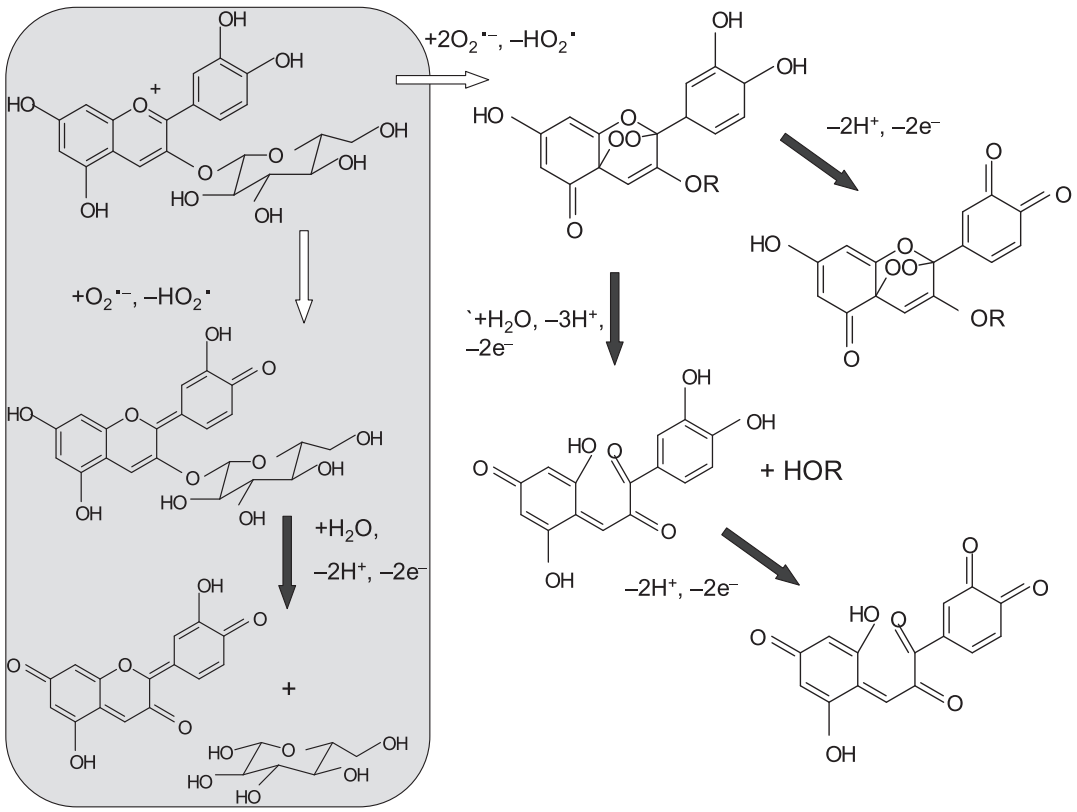

Fig. 5. Scheme of the redox processes involved in the ROS-assisted electrochemistry of anthocyanins for cyanidin 3-glucoside. The grey zone marks the pathway followed for generating signals II in the voltammograms, whereas the white region corresponds to the signals I in the voltammograms. Here, the glucoside unit has been abbreviated as OR. Dark grey arrows: electrochemical processes; white arrows: chemical reaction processes.

For our purposes, the relevant point to note is that the essentially unexplored electrochemistry of anthocyanins in the presence of electrochemically generated ROS involves the generation of new electroactive species with very negative oxidation potentials. According to the tentative scheme in Fig. 5, such generated species could be oxidized to species with considerable electron conjugation. This is consistent with their expected relatively high stability, which at the first glance justifies their very negative oxidation potentials, i.e., their high antioxidant capacity.

These results introduce a new scenario in the chemistry of anthocyanins where the reaction with ROS could operate via the conventional pathway, via semiquinone species (related to I signals) and/or via ROS activation of species with high antioxidant capacity (related to the II signals). Although much research is needed to explore this complex picture, the above electrochemical results suggest that there is a ROS-assisted promotion of the antioxidant role of anthocyanins. In terms of plant physiology, this implies that ROS may not only act as signal transducers, but also as activators of the antioxidant properties of anthocyanins.

These results are of interest in the field of food chemistry because they validate the possibility of generating anthocyanin-derived species with high antioxidant capacity in foods and confirm the preservation of these properties under lyophilization. These properties open up potential new strategies for food production and conservation through modulation of ROS reactivity.

4. Conclusions

The voltammetric response of microparticulate deposits obtained from the ethanolic extracts of lyophilized specimens of blueberry and raspberry samples in contact with aqueous electrolytes differs significantly in the presence and in the absence of dissolved oxygen. This voltammetry is dominated by anodic processes occurring between 0.0 and 1.2 V vs. Ag/AgCl mainly corresponding to the oxidation of *o*-catechol units to *o*-quinone units of anthocyanins (especially cyanidin and peonidin glucosides in particular). These are accompanied, in the presence of oxygen under conditions of electrochemical ROS generation, by new oxidation peaks at high negative values (ca. − 0.7 V vs. Ag/AgCl), corresponding to anthocyanin-derived species with high antioxidant capacity.

The voltammetric pattern, in agreement with the SECM study of the epithelial deposits of the fruits, suggests that there is a ROS activation of the antioxidant capacity of the anthocyanins. Accordingly, reaction schemes can be proposed that yield anthocyanin-derived species with high degree of electronic conjugation and increased antioxidant capacity.

CRediT authorship contribution statement

Irene Domínguez: Conceptualization, Data curation, Formal analysis. **Irene Romero:** Data curation, Formal analysis. **M. Teresa Sanchez-Ballesta:** Data curation, Formal analysis. **M. Isabel Escribano:** Data curation, Formal analysis. **Carmen Merodio:** Data curation, Formal analysis. **Antonio Doménech-Carbó:** Conceptualization, Data curation, Formal analysis.

Declaration of Competing Interest

The authors declare that they have no known competing financial interests or personal relationships that could have appeared to influence the work reported in this paper.

Data availability

Data will be made available on request.

Acknowledgments

Financial support by the projects PID2020-113965RB-I00/AEI/ 10.13039/501100011033 and Grant PID2020-113022GB-I00 funded by MCIN/AEI/ 10.13039/501100011033 and by "ERDF A way of making Europe", by the "European Union frame is gratefully acknowledged.

Appendix A. Supplementary material

Supplementary data to this article can be found online at https://doi.org/10.1016/j.foodchem.2023.137649.

References

Arroyo-Currás, N., Rosas-García, V. M., & Videa, M. (2016). Substituent Inductive Effects on the Electrochemical Oxidation of Flavonoids Studied by SquareWave Voltammetry and Ab Initio Calculations. *Molecules, 21*, 1422.

Cerqueira, J. V. A., de Andrade, M. T., Rafeal, D. D., Zhu, F., Martins, S. V. C., Nunes-Nesi, A., … Zsögön, A. (2023). Anthocyanins and reactive oxygen species: A team of rivals regulating plant development? *Plant Molecular Biology, 112*, 213–223.

Cesa, S., Carradori, S., Bellagamba, G., Locatelli, M., Casadei, M. A., Masci, A., & Paolicelli, P. (2017). Evaluation of processing effects on anthocyanin content and colour modifications of blueberry (Vaccinium spp.) extracts: Comparison between HPLC-DAD and CIELAB analyses. *Food Chemistry, 232*, 114–123.

De Lima, A. A., Sussuchi, E. M., & De Giovanni, W. F. (2007). Electrochemical and Antioxidant Properties of Anthocyanins and Anthocyanidins. *Croatica Chemica Acta, 80*, 29–34.

Dimitrić Marković, J. M., Pejin, B., Milenković, D., Amić, D., Begović, N., Mojović, M., & Marković, Z. S. (2017). Antiradical activity of delphinidin, pelargonidin and malvin towards hydroxyl and nitric oxide radicals: The energy requirements calculations as a prediction of the possible antiradical mechanisms. *Food Chemistry, 218*, 440–446.

Doménech-Carbó, A., & Domínguez, I. (2023). In situ electrochemical analysis of anthocyanin activation by ROS in blueberries. *Electrochemistry Communications, 149*, Article 107468.

Doménech-Carbó, A., Ibars, A. M., Prieto-Mossi, J., Estrelles, E., Scholz, F., Cebrián-Torrejón, G., & Martini, M. (2015). Electrochemistry-based chemotaxonomy in plants using the voltammetry of microparticles methodology. *New Journal of Chemistry, 39*, 7421–7428.

Doménech-Carbó, A., Domínguez, I., Hernández-Muñoz, P., & Gavara, R. (2015). Electrochemical tomato (Solanum lycopersicum L.) characterization using contact probe in situ voltammetry. *Food Chemistry, 127*, 318–325.

Doménech-Carbó, A., Gavara, R., Hernández-Muñoz, P., & Domínguez, I. (2015). Contact probe voltammetry for in situ monitoring of the reactivity of phenolic tomato (Solanum lycopersicum L.) compounds with ROS. *Talanta, 144*, 1207–1215.

Doménech-Carbó, A., Dias, D., & Donnici, M. (2021). In vivo electrochemical monitoring of signaling transduction of plant defense against stress in leaves of Aloe vera L. *Electroanalysis, 33*, 1024–1032.

Doménech-Carbó, A., Labuda, J., & Scholz, F. (2013). Electroanalytical chemistry for the analysis of solids: characterization and classification (IUPAC Technical Report). *Pure and Applied Chemistry, 85*, 609–631.

Doménech-Carbó, A., Montoya, N., Soriano, P., & Estrelles, E. (2018). An electrochemical analysis suggests role of gynodioecy in adaptation to stress in *Cortaderia selloana*. *Current Plant Biology, 16*, 9–14.

Dong, R., Tian, J., Huang, Z., Yu, Q., Xie, J., Li, B., … Chen, Y. (2023). Intermolecular binding of blueberry anthocyanins with water-soluble polysaccharides: Enhancing their thermostability and antioxidant abilities. *Food Chemistry, 410*, Article 135375.

Duan, C., Xiao, X., Yu, Y., Xu, M., Zhang, Y., Liu, X., … Wang, J. (2024). In situ Raman characterization of the stability of blueberry anthocyanins in aqueous solutions under perturbations in temperatura. UV, pH. *Food Chemistry, 431*, Article 137155.

Fan, L., Lin, L., Zhang, Y., Li, S., & Tang, Z. (2023). Component characteristics and reactive oxygen species scavenging activity of anthocyanins from fruits of *Lonicera caerulea*. *Food Chemistry, 403*, Article 134391.

Garcia, C., & Blesso, C. N. (2021). Antioxidant properties of anthocyanins and their mechanism of action in atherosclerosis. *Free Radical Biology and Medicine, 20*, 152–166.

Herscu-Kluska, R., Masanwa, A., Saphier, M., Cohen, H., & Meverstein, D. (2008). Mechanism of the reaction of radicals with peroxides and dimethyl sulfoxide in aqueous solution. *Chemistry, 14*, 5880–5890.

Jadreško, D., Miličević, A., & Novak Jovanović, I. (2022). Reactivity of flavonoids toward superoxide radical: An electrochemical approach. *Electrochimica Acta, 421*, Article 140501.

Janeiro, P., & Oliviera-Brett, A. M. (2007). Redox Behavior of Anthocyanins Present in Vitis vinifera L. *Electroanalysis, 19*, 1779–1786.

Karnicka, K., Eckhard, K., Guschin, D. A., Stoica, L., Kulesza, P. J., & Schumann, W. (2007). Visualisation of the local bio-electrocatalytic activity in biofuel cell cathodes by means of redox competition scanning electrochemical microscopy (RC-SECM). *Electrochemistry Communications, 9*, 1998–2002.

Katsounaros, I., Schneider, W. B., Meier, J. C., Benedikt, U., Biedermann, P. U., Auer, A. A., & Mayrhofer, K. J. (2012). Hydrogen peroxide electrochemistry on platinum: Towards understanding the oxygen reduction reaction mechanism. *PhysChemChemPhys, 14*, 7384–7391.

Kim, A.-N., Lee, K.-Y., Kim, B. G., Cha, S. W., Jeong, E. J., Kerr, W. L., & Choi, S. G. (2021). Thermal processing under oxygen–free condition of blueberry puree: Effect on anthocyanin, ascorbic acid, antioxidant activity, and enzyme activities. *Food Chemistry, 342*, Article 128345.

Krishnamachari, V., Levine, L. H., & Paré, P. W. (2002). Flavonoid oxidation by the radical generator AIBN: A unified mechanism for quercetin radical scavenging. *Journal of Agricultural and Food Chemistry, 50*, 4357–4363.

Lang, Y., Li, B., Gong, E., Shu, C., Si, X., Gao, N., … Meng, X. (2021). Effects of α-casein and β-casein on the stability, antioxidant activity and bioaccessibility of blueberry anthocyanins with an *in vitro* simulated digestion. *Food Chemistry, 334*, Article 127526.

Lauw, S. J. L., Chiang, Z., Lee, J. H. Q., & Webster, R. D. (2018). Comparing the Relative Reactivities of Structurally Varied Alcohols toward Electrochemically Generated Superoxide. *ChemElectroChem, 5*, 643–650.

Litwinienko, G., & Ingold, K. U. (2007). Solvent effects on the rates and mechanisms of reaction of phenols with free radicals. *Accounts of Chemical Research, 40*, 222–230.

Masek, A., Chrzescijanska, R., & Zaborski, M. (2014). Electrooxidation of morin hydrate at a Pt electrode studied by cyclic voltammetry. *Food Chemistry, 148*, 18–23.

Mateo, E. M., Gómez, J. V., Montoya, N., Mateo-Castro, R., Gimeno-Adelantado, J. V., Jiménez, M., & Doménech-Carbó, A. (2018). Electrochemical identification of toxigenic fungal species using solid-state voltammetry strategies. *Food Chemistry, 267*, 91–100.

Mihailović, N. R., Mihailović, V. B., Ćirić, A. R., Srecković, N. Z., Cvijković, M. R., & Joksović, L. G. (2019). Analysis of Wild Raspberries (Rubus idaeus L.): Optimization of the Ultrasonic-Assisted Extraction of Phenolics and a New Insight in Phenolics Bioaccessibility. *Plant Foods for Human Nutrition, 74*, 399–404.

Mustafa, A. M., Angeloni, S., Abouelenein, D., Acquaticci, L., Xiao, J., Sagratini, G., … Caprioli, G. (2022). A new HPLC-MS/MS method for the simultaneous determination of 36 polyphenols in blueberry, strawberry and their commercial products and determination of antioxidant activity. *Food Chemistry, 367*, Article 130743.

Olson, K. R., Gao, Y., Briggs, A., Devireddy, N., Iovino, N. A., Licursi, M., … Straub, K. D. (2021). 'Antioxidant' berries, anthocyanins, resveratrol and rosmarinic acid oxidize hydrogen sulfide to polysulfides and thiosulfate: A novel mechanism underlying their biological actions. *Free Radical Biology and Medicine, 165*, 67–78.

Ramesova, S., Sokolova, R., Tarabek, J., & Degano, I. (2013). The oxidation of luteolin, the natural flavonoid dye. *Electrochimica Acta, 110*, 646–654.

Sadilova, E., Stintzing, F. C., & Carle, R. (2006). Thermal Degradation of Acylated and Nonacylated Anthocyanins. *Journal of Food Science, 71*, C504–C512.

Scholz, F., & Meyer, B. (1998). *Voltammetry of solid microparticles immobilized on electrode surfaces, in Electroanalytical Chemistry, A Series of Advances, 20* pp. 1–86). New York: Marcel Dekker.

Scholz, F., Schröder, U., Gulabowski, R., & Doménech-Carbó, A. (2014). *Electrochemistry of Immobilized Particles and Droplets* (2nd ed.). Berlin-Heidelberg: Springer.

Shi, J., Xiao, Y., Jia, C., Zhang, H., Gan, Z., Li, X., … Wang, Q. (2023). Physiological and biochemical changes during fruit maturation and ripening in highbush blueberry (Vaccinium corymbosum L.). *Food Chemistry, 410*, Article 135299.

Sinopoli, A., Calogero, G., & Bartolotta, A. (2019). Computational aspects of anthocyanidins and anthocyanins: A review. *Food Chemistry, 297*, Article 124898.

Slika, H., Manssur, H., Wehbe, N., Nasser, S. A., Iratni, R., Nasrallah, G., … Eid, A. H. (2022). Therapeutic potential of flavonoids in cancer: ROS-mediated mechanisms. *Biomedicine & Pharmacotherapy, 146*, Article 112442.

Wasternack, C., & Hause, B. (2013). Jasmonates: Biosynthesis, perception, signal transduction and action in plant stress response, growth and development. An update to the 2007 review in Annals of Botany. *Annals of Botany, 111*, 1021–1058.

Xu, J., Huang, W., & McCreery, R. L. (1996). Isotope and surface preparation effects on alkaline dioxygen reduction at carbon electrodes. *Journal of Electroanalytical Chemistry, 410*, 235–242.

Yang, L., Yang, T., Li, G., Ma, J. x., & Yu, Y. (2022). Electrochemical Studies of Polyphenols, Anthocyanins, and Flavonoids Extracted from Blueberry Fruit. *International Journal of Electrochemical Science, 17*, 22038.

Yi, L., Chen, C. –y., Jin, X., Zhang, T., Zhou, Y., Zhang, Q. –y., Zhu, J. d. & Mi, M. –t. (2012). Differential suppression of intracellular reactive oxygen species-mediated signaling pathway in vascular endothelial cells by several subclasses of flavonoids. *Biochimie, 94*, 2035–2044.

Zhou, J.-Y., Li, X., Zhao, D., Deng-Wang, M.-Y., & Dai, C.-C. (2016). Reactive oxygen species and hormone signaling cascades in endophytic bacterium induced essential oil accumulation in Atractylodes lancea. *Planta, 244*, 699–712.